BER and Diversity Order Analysis of Distributed Alamouti's Code with CSI-Assisted Relays

Zhihang Yi, MinChul Ju, Hyoung-Kyu Song, and Il-Min Kim, *Senior Member, IEEE*

***Abstract*—This paper focuses on the average bit error rate (BER) and diversity order analysis of the distributed Alamouti's code in dissimilar cooperative networks with channel state information (CSI)-assisted relays. We first assume that the relays adopt the amplifying coefficient proposed in [1]. Lower and upper bounds of the average BER of the distributed Alamouti's code are derived. Those two bounds tightly bound the exact average BER. Then we show that, surprisingly, the distributed Alamouti's code achieves only diversity order one when the relays use the amplifying coefficient proposed in [1]. To resolve this problem, we propose a new threshold-based amplifying coefficient for the distributed Alamouti's code based on the work in [3]. This new amplifying coefficient makes the distributed Alamouti's code achieve the full diversity order two. Moreover, based on three different CSI assumptions, four amplifying schemes are developed in order to determine the value of the threshold used in the new amplifying coefficient.**

***Index Terms*—Bit error rate (BER), channel state information (CSI)-assisted relay, distributed Alamouti's code, diversity order.**

I. Introduction

In a cooperative network, several single-antenna relay terminals help the source transmit signals to the destination by virtually forming a distributed multiple-antenna system [1]–[5]. Specifically, in an amplify-and-forward (AF) cooperative network, each relay multiplies the received signal with an amplifying coefficient and then forwards it to the destination. In order to coordinate the transmissions from the relays, *distributed space-time block codes* (DSTBCs) have been proposed and extensively studied [2], [6] and [7]. Many works have analyzed the error performance and diversity order of the DSTBCs in AF cooperative networks. For example, Jing *et al.* showed that the DSTBCs could achieve the full diversity order in the number of relays [2]. In [8], Ju *et al.* found the exact average BER expression of the distributed Alamouti's code; but the expression was not given in closed-form. Very recently, two closed-form approximate average BER expressions were derived for the distributed Alamouti's code [9].

However, the authors of [2], [8], and [9] all assumed that the relays in the cooperative network did not have any channel side information (CSI) of the first-hop channels, i.e. the channels from the source to the relays. Those relays were called the *blind relays* in the literature. As a result, the amplifying coefficients at the relays were fixed constants, and the power efficiency significantly deteriorated because the power amplifier at each relay might operate in the non-linear region when the instantaneous gains of the first-hop channels were large [10]. In practical systems, it is more preferable to implement the *CSI-assisted relays* which know the instantaneous channel gains of the first-hop channels. In fact, this CSI can be easily obtained at the relays without any feedback overhead. Laneman *et al.* have proposed an amplifying coefficient for the CSI-assisted relays [1] and it can successfully enhance the power efficiency at the relays [10]. Due to this reason, this amplifying coefficient has been used in numerous previous publications [11]–[13]. Therfore, it is practically very important to analyze the distributed Alamouti's code in cooperative networks with CSI-assisted relays. Because it is very hard to directly extend the results in [2], [8], and [9] to such networks, a new approach must be taken.

In this paper, we analyze the error performance and diversity order of the distributed Alamouti's code with CSI-assisted relays. Specifically, we first consider a *dissimilar* cooperative network, where all the channels possibly have different variances, and we assume that the CSI-assisted relays in the network adopt the amplifying coefficient proposed in [1]. We derive lower and upper bounds of the average BER of the distributed Alamouti's code. Irrespective of the values of the channel variances, the proposed bounds tightly bound the average BER. Very surprisingly, we find that, when the relays use the amplifying coefficient proposed in [1], the distributed Alamouti's code achieves only diversity order one. To address this problem, we then propose a new threshold-based amplifying coefficient for the distributed Alamouti's code based on the work in [3]. This new amplifying coefficient makes the code achieve the full diversity order two. Moreover, it also enhances the power efficiency at the relays. Based on three different CSI assumptions, we develop four amplifying schemes in order to determine the value of the threshold used in the new amplifying coefficient.

The rest of this paper is organized as follows. Section II describes the cooperative network studied in this paper. In Section III, assuming that the relays adopt the amplifying

Manuscript received March 12, 2010; revised July 30, 2010; accepted January 21, 2011. The associate editor coordinating the review of this paper and approving it for publication was H.-C. Yang.

This research was supported in part by the Natural Sciences and Engineering Research Council of Canada (NSERC), and by the Ubiquitous Computing and Network (UCN) Project, Knowledge and Economy Frontier R&D Program of the Ministry of Knowledge Economy (MKE) in Korea as a result of UCNs subproject 10C2-C2-12T.

Z. Yi and I.-M. Kim are with the Department of Electrical and Computer Engineering, Queen's University, Kingston, ON, Canada, K7M 2A8 (e-mail: zhihang.yi@gmail.com, ilmin.kim@queensu.ca).

M. Ju was with the Department of Electrical and Computer Engineering, Queen's University, Kingston, Ontario, Canada. He is now with Korea Electronics Technology Institute (KETI), Seoul, Korea (e-mail: mcju@keti.re.kr).

H.-K. Song is with the Department of Information and Communication Engineering, Sejong University, Seoul, Korea (e-mail: songhk@sejong.ac.kr).

Digital Object Identifier 10.1109/TWC.2011.020811.100375

coefficient proposed in [1], we derive lower and upper bounds of the average BER of the distributed Alamouti's code in a dissimilar cooperative network. Furthermore, we show that the diversity order of the distributed Alamouti's code is just one when the relays use the amplifying coefficient proposed in [1]. In Section IV, a new threshold-based amplifying coefficient is proposed. This new amplifying coefficient makes the distributed Alamouti's code achieve the full diversity order two. Moreover, we develop four amplifying schemes in order to determine the value of the threshold used by the new amplifying coefficient. Section V presents some numerical results and Section VI concludes this paper.

Notation: We use $A := B$ to denote A, by definition, equals B and use $A =: B$ to denote B, by definition, equals A. For a random variable X, $\mathrm{E}[X]$ denotes its expectation. $X \sim \mathcal{CN}(0, \Omega_X)$ means X is a circularly symmetric complex Gaussian random variable with zero mean and variance Ω_X. Let $\lfloor \cdot \rfloor$, $Q(\cdot)$, ${}_2F_1(1, 2; 3; \cdot)$, and $\mathrm{Ei}(\cdot)$ denote the floor function, Q-function, hypergeometric function, and exponential integral function [15], respectively.

II. System Description

In this section, we first describe the system model, and then discuss two possible relaying coefficients: a blind relaying coefficient and a CSI-assisted relaying coefficient.

A. System Model and Distributed Alamouti's Code

We consider an AF cooperative network with one source, two CSI-assisted relays, and one destination. Every terminal has only one antenna and is half-duplex. We use S, D, and R_k to denote the source, the destination, and the k-th relay for $k = 1, 2$, respectively. Let h_k and f_k denote the channel from S to R_k and the channel from R_k to D, respectively. The channel coefficient h_k is modeled as $h_k = \bar{h}_k \sqrt{d_{s,k}^{-\beta_{s,k}}}$, where $\bar{h}_k \sim \mathcal{CN}(0, 1)$, $\beta_{s,k}$ is the path loss exponent for this channel, and $d_{s,k}$ is the normalized distance between S and R_k. The value of $d_{s,k}$ is decided by $d_{s,k} = \bar{d}_{s,k}/D$, where $\bar{d}_{s,k}$ is the actual distance between S and R_k and D is the reference distance determined from measurements [16]. Similarly, we model the channel coefficient f_k as $f_k = \bar{f}_k \sqrt{d_{k,d}^{-\beta_{k,d}}}$, where $d_{k,d}$ is the normalized distance between R_k and D, $\beta_{k,d}$ is the path loss exponent for this channel, and $\bar{f}_k \sim \mathcal{CN}(0, 1)$. The value of $d_{k,d}$ is decided by $d_{k,d} = \bar{d}_{k,d}/D$, where $\bar{d}_{k,d}$ is the actual distance between R_k and D. Thus, the variances Ω_{h_k} and Ω_{f_k} of h_k and f_k equal to $\Omega_{h_k} = d_{s,k}^{-\beta_{s,k}}$ and $\Omega_{f_k} = d_{k,d}^{-\beta_{k,d}}$, respectively.

The system model for the distributed Alamouti's code is depicted in Fig. 1. Specifically, at the first and second time slots, S transmits two information-bearing symbols x_1 and x_2 to R_1 and R_2, respectively. The transmission power at S is E_s. The received signal $y_{k,t}$ of R_k at the t-th time slot is given by $y_{k,t} = \sqrt{E_s} h_k x_t + n_{k,t}$ for $k = 1, 2$ and $t = 1, 2$, where $n_{k,t}$ is the additive white Gaussian noise and $n_{k,t} \sim \mathcal{CN}(0, \sigma_n^2)$.

At the third and fourth time slots, the two relays use the distributed Alamouti's code to transmit signals to the destination after multiplying the received signal $y_{k,t}$ with an amplifying coefficient ρ_k. The coefficient ρ_k will be discussed in detail later. Specifically, at the third time slot, R_1 transmits $\rho_1 y_{1,1}$ and R_2 transmits $-\rho_2 y_{2,2}^*$. Thus, the received signal at D is $y_1 = \rho_1 f_1 y_{1,1} - \rho_2 f_2 y_{2,2}^* + n_1$, where n_1 is the additive white Gaussian noise and $n_1 \sim \mathcal{CN}(0, \sigma_n^2)$. At the fourth time slot, R_1 transmits $\rho_1 y_{1,2}$ and R_2 transmits $\rho_2 y_{2,1}^*$. Consequently, the received signal at D is $y_2 = \rho_1 f_1 y_{1,2} + \rho_2 f_2 y_{2,1}^* + n_2$, where n_2 is the additive white Gaussian noise and $n_2 \sim \mathcal{CN}(0, \sigma_n^2)$. Due to the orthogonal structure of the distributed Alamouti's code, the maximum likelihood (ML) estimate $\hat{x}_1$ of x_1 is given by $\hat{x}_1 = \rho_1 f_1^* h_1^* y_1 + \rho_2 f_2 h_2^* y_2^*$ [8]. Thus, the instantaneous SNR $\gamma(\rho_1, \rho_2)$ of $\hat{x}_1$ is given by

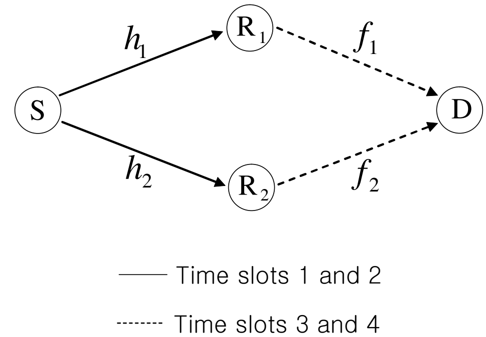

Fig. 1. System model for the distributed Alamouti's code.

$$\gamma(\rho_1, \rho_2) = \frac{E_s(\rho_1^2 |f_1 h_1|^2 + \rho_2^2 |f_2 h_2|^2)}{\sigma_n^2(\rho_1^2 |f_1|^2 + \rho_2^2 |f_2|^2 + 1)}. \tag{1}$$

Similarly, the instantaneous SNR of the ML estimate $\hat{x}_2$ of x_2 is also given by $\gamma(\rho_1, \rho_2)$.

If M-quadrature amplitude modulation (QAM) is used as the modulation scheme, the exact closed-form BER $P_b(\gamma(\rho_1, \rho_2))$, conditioned on the instantaneous channel coefficients h_k and f_k, of $\hat{x}_1$ or $\hat{x}_2$ is given by [17][1]

$$P_b\left(\gamma(\rho_1, \rho_2)\right) = \frac{2}{\sqrt{M}\log_2 M} \sum_{j=1}^{\log_2 \sqrt{M}} \left[\sum_{i=0}^{(1-2^{-j})\sqrt{M}-1} A_{j,i}(M) \times Q\left((2i+1)\sqrt{\frac{3\gamma(\rho_1, \rho_2)}{M-1}} \right) \right], \tag{2}$$

where the coefficient $A_{j,i}(M)$ is given by

$$A_{j,i}(M) = (-1)^{\left\lfloor 2^{j-1} i / M \right\rfloor} \left(2^{j-1} - \left\lfloor \frac{2^{j-1} i}{\sqrt{M}} + \frac{1}{2} \right\rfloor \right). \tag{3}$$

The average BER P_b can be obtained by $P_b = \mathrm{E}\left[P_b(\gamma(\rho_1, \rho_2))\right]$, i.e.

$$P_b = \frac{2}{\sqrt{M}\log_2 M} \sum_{j=1}^{\log_2 \sqrt{M}} \left\{ \sum_{i=0}^{(1-2^{-j})\sqrt{M}-1} A_{j,i}(M) \times \mathrm{E}\left[Q\left((2i+1)\sqrt{\frac{3\gamma(\rho_1, \rho_2)}{M-1}} \right) \right] \right\}. \tag{4}$$

[1]If other modulation schemes are used, the conditional BER can be obtained by using [17] as well.

B. Blind Relaying and CSI-Assisted Relaying Coefficients

In this subsection, we discuss two widely-adopted relaying coefficients: a blind relaying coefficient and a CSI-assisted relaying coefficient. We first consider the blind relaying coefficient. In the blind relaying, a fixed amplifying coefficient $\rho_k = \sqrt{c_k}$ is used, where c_k is a positive constant [2], [8], and [9]. When this ρ_k is used, the performance of the distributed Alamouti's code has been extensively studied in the literature [8], [9]. In particular, it has been shown that the distributed Alamouti's code achieved the full diversity order two. This blind relaying coefficient, however, raises a problem that the output power at the relay is given by $c_k(E_s|h_k|^2+\sigma_n^2)$, which varies substantially with time due to $|h_k|^2$. Particularly, the peak-to-average power ratio (PAPR) can be practically very large or it can be theoretically even infinity[2] depending on the distribution of $|h_k|^2$. Thus, the power efficiency significantly deteriorates, because the power amplifier at each relay operates in the non-linear region when $|h_k|^2$ is large. It is well-known that the power efficiency deteriorates when the power amplifier operates in the non-linear region [14].

Another well-known amplifying coefficient is the CSI-assisted relaying coefficient. In the CSI-assisted relaying, the amplifying coefficient ρ_k is given by [1]

$$\rho_k = \sqrt{\frac{E_{rk}}{E_s|h_k|^2 + \sigma_n^2}}. \tag{5}$$

A benefit of this amplifying coefficient is that the output power of the k-th relay is always maintained to be E_{rk}, and thus, the PAPR is 0 dB. Hence, this CSI-assisted relaying is very practical, because the power amplifier at each relay will never go into the non-linear region. Due to this reason, the amplifying coefficient ρ_k of (5) has been used in numerous previous publications [11]–[13]. However, the performance of the distributed Alamouti's code with ρ_k of (5) has not been well-studied in the literature. In this paper, focusing on ρ_k of (5), we will derive average BER of the distributed Alamouti's code and show that, very surprisingly, the distributed Alamouti's code achieves only diversity order one.

III. BER and Diversity Order Analysis of the Distributed Alamouti's Code

In this section, adopting the CSI-assisted relaying coefficient ρ_k in (5), we first derive lower and upper bounds of the average BER of the distributed Alamouti's code. Then we show that, very surprisingly, the distributed Alamouti's code achieves only diversity order one.

In order to facilitate the analysis of the average BER P_b, we approximate ρ_k by $\rho_k \approx \sqrt{E_{rk}/(E_s|h_k|^2)}$ as in [11] and [12]. Note that $\sqrt{E_{rk}/(E_s|h_k|^2)}$ is a very tight approximation of ρ_k as shown in [11] and [12]. For example, in [11], it has been demonstrated that the difference between the exact average BER and the approximate average BER, which is based on the approximation $\rho_k \approx \sqrt{E_{rk}/(E_s|h_k|^2)}$, is less than 0.2 dB.

[2]The PAPR is defined as the ratio of the maximum transmission power $E_{\max}$ to the average transmission power E_{avg}, i.e. $\text{PAPR} := E_{\max}/E_{\text{avg}}$. For the blind relaying, the PAPR at the k-th relay is given by $\text{PAPR} = E_{\max}/E_{\text{avg}} = c_k(E_s \max[|h_k|^2] + \sigma_n^2)/(c_k(E_s \mathrm{E}[|h_k|^2] + \sigma_n^2))$. In this case, the PAPR can be infinity if $\max[|h_k|^2]$ is infinity.

Therefore, the instantaneous SNR $\gamma(\rho_1,\rho_2)$ in (1) is tightly approximated by

$$\gamma(\rho_1,\rho_2) \approx \frac{1}{\sigma_n^2}\frac{E_{r1}|f_1|^2 + E_{r2}|f_2|^2}{\frac{E_{r1}|f_1|^2}{E_s|h_1|^2} + \frac{E_{r2}|f_2|^2}{E_s|h_2|^2} + 1}. \tag{6}$$

Now we will analyze the average BER P_b based on (6). It is well-known that the moment generating function (MGF)-based approach is very useful to derive P_b for various constellations [18]. In order to obtain the value of P_b, one needs the MGF of $\gamma(\rho_1,\rho_2)$, which is technically very hard. In the following, we try to find lower and upper bounds of P_b and show that the bounds are very tight to P_b.

A. A lower bound of P_b

We upper-bound $\gamma(\rho_1,\rho_2)$ in the following way

$$\gamma(\rho_1,\rho_2) < \gamma^U = \frac{1}{\sigma_n^2}\frac{E_{r1}|f_1|^2 + E_{r2}|f_2|^2}{\max\left(\frac{E_{r1}|f_1|^2}{E_s|h_1|^2}, \frac{E_{r2}|f_2|^2}{E_s|h_2|^2}\right)}. \tag{7}$$

In order to find a lower bound of P_b, it is desirable to obtain the MGF of γ^U. To this end, we prove the following lemma.

Lemma 1: Assume X_1, X_2, Y_1, and Y_2 are exponential random variables with means a_1, a_2, b_1, and b_2, respectively. The MGF $\mathcal{M}_1(s; a_1, a_2, b_1, b_2)$ of the function $(Y_1 + Y_2)/\max(Y_1/X_1, Y_2/X_2)$ is given as follows:

$$\mathcal{M}_1(s;a_1,a_2,b_1,b_2) = \frac{b_1 b_2}{a_1 a_2}\left(\frac{a_1 - a_2}{b_1 - b_2}\mathcal{M}_1^1(s;a_1,a_2,b_1,b_2) + \frac{a_2 b_1 - a_1 b_2}{b_1 - b_2}\mathcal{M}_1^2(s;a_1,a_2,b_1,b_2)\right). \tag{8}$$

In this function, $\mathcal{M}_1^1(s;a_1,a_2,b_1,b_2)$ and $\mathcal{M}_1^2(s;a_1,a_2,b_1,b_2)$ are given by

$$\mathcal{M}_1^1(s;a_1,a_2,b_1,b_2) = \frac{a_1 a_2}{a_1 b_2(1-a_2 s) - a_2 b_1(1-a_1 s)} \ln \frac{a_1 b_2(1-a_2 s)}{a_2 b_1 (1-a_1 s)}, \tag{9}$$

$$\begin{aligned}\mathcal{M}_1^2(s;a_1,a_2,b_1,b_2) &= \frac{a_1}{b_2(b_1-b_2)(1-a_1 s)} - \frac{a_2}{b_1(b_1-b_2)(1-a_2 s)} \\ &+ \frac{a_2(a_1-a_2)}{2a_1(1-a_2 s)^2(b_2-b_1)^2}\ {}_2F_1\left(1,2;3;\frac{\frac{a_2 b_1 - a_1 b_2}{a_1(b_1-b_2)} - a_2 s}{1-a_2 s}\right) \\ &+ \frac{a_1(a_2-a_1)}{2a_2(1-a_1 s)^2(b_1-b_2)^2}\ {}_2F_1\left(1,2;3;\frac{\frac{a_2 b_1 - a_1 b_2}{a_2(b_1-b_2)} - a_1 s}{1-a_1 s}\right).\end{aligned} \tag{10}$$

Proof: See Appendix A. □

Using Lemma 1, the MGF $\mathcal{M}^U(s)$ of γ^U can now be easily derived, and it is given by

$$\mathcal{M}^U(s) = \mathcal{M}_1\left(\frac{s}{\sigma_n^2}; E_s\Omega_{h_1}, E_s\Omega_{h_2}, E_{r_1}\Omega_{f_1}, E_{r_2}\Omega_{f_2}\right). \tag{11}$$

Based on (11), we obtain a lower bound of P_b in the following theorem.

Theorem 1: When M-QAM is used as the modulation scheme, the average BER P_b can be lower-bounded by

$$P_b > P_b^L = \frac{2}{\pi\sqrt{M}\log_2 M} \sum_{j=1}^{\log_2\sqrt{M}} \left\{ \sum_{i=0}^{(1-2^{-j})\sqrt{M}-1} A_{j,i}(M) \times \int_{\theta=0}^{\frac{\pi}{2}} \mathcal{M}^U\left(-\frac{3(2i+1)^2}{2(M-1)\sin^2\theta}\right) d\theta \right\}. \quad (12)$$

Proof: Since $\gamma(\rho_1,\rho_2)$ is upper-bounded by γ^U and the MGF of γ^U is given by $\mathcal{M}^U(s)$ in (11), it follows Craig's formula [18, eq. (4.2)] that

$$\mathrm{E}\left[Q\left((2i+1)\sqrt{\frac{3\gamma(\rho_1,\rho_2)}{M-1}}\right)\right] > \frac{1}{\pi}\int_{\theta=0}^{\frac{\pi}{2}} \mathcal{M}^U\left(-\frac{3(2i+1)^2}{2(M-1)\sin^2\theta}\right) d\theta. \quad (13)$$

By substituting (13) into (4), we obtain the lower bound P_b^L. □

Although the lower bound P_b^L contains an integration, this integration is over a finite range, and hence, it is not hard to compute. In fact, it is well-known that Q-function can be approximated by $\frac{1}{12}e^{-x^2/2} + \frac{1}{4}e^{-2x^2/3}$ [19]. By using this approximation, we can obtain approximate P_b^L in *closed-form*, which can further reduce the computational complexity. Numerical results will demonstrate that P_b^L is a very tight lower bound of P_b except when Ω_{h_k} is much larger than Ω_{f_k}. For this special case, the ratio $E_{rk}|f_k|^2/(E_s|h_k|^2)$ in the denominator of (6) is much smaller than one with a very high probability. Therefore, P_b^L loses its tightness because we neglect the constant one in the denominator of $\gamma(\rho_1,\rho_2)$ as shown in (7) when we derive P_b^L. This particular case will be addressed by deriving an upper bound of P_b in the next subsection.

B. An upper bound of P_b

In order to find a tight bound for P_b when Ω_{h_k} is much larger than Ω_{f_k}, we develop an upper bound of P_b in the following. We keep the constant one in the denominator of $\gamma(\rho_1,\rho_2)$; but replace $|h_1|^2$ and $|h_2|^2$ by $\min(|h_1|^2,|h_2|^2)$. This gives us a lower bound γ^L of $\gamma(\rho_1,\rho_2)$

$$\gamma(\rho_1,\rho_2) \geq \gamma^L = \frac{1}{\sigma_n^2}\frac{E_{r1}|f_1|^2 + E_{r2}|f_2|^2}{\frac{E_{r1}|f_1|^2+E_{r2}|f_2|^2}{E_s\min(|h_1|^2,|h_2|^2)}+1}. \quad (14)$$

In order to find an upper bound of P_b, it is desirable to obtain the MGF of γ^L. Thus, we show the following lemma.

Lemma 2: Assume X_1, X_2, Y_1, and Y_2 are exponential random variables with means a_1, a_2, b_1, and b_2, respectively. The MGF $\mathcal{M}_2(s;a_1,a_2,b_1,b_2)$ of the function $(Y_1+Y_2)/((Y_1+Y_2)/\min(X_1,X_2)+1)$ is given as follows:

$$\mathcal{M}_2(s;a_1,a_2,b_1,b_2) = \frac{b_1}{b_1-b_2}W\left(s,\frac{a_1a_2}{a_1+a_2},b_1\right) - \frac{b_2}{b_1-b_2}W\left(s,\frac{a_1a_2}{a_1+a_2},b_2\right), \quad (15)$$

where the function $W(x,y,z)$ is given by

$$W(x,y,z) = \frac{1}{(y+z-xyz)^2-4yz}\Bigg[(y+z)(y+z-xyz) - 4yz + \frac{4yz(-xyz)\sqrt{(y+z-xyz)^2}}{(y+z-xyz)\sqrt{4yz-(y+z-xyz)^2}} \times \arccos\left(\frac{y+z-xyz}{2\sqrt{yz}}\right)\Bigg]. \quad (16)$$

Proof: Let $T = Y_1+Y_2$ and $Z=\min(X_1,X_2)$. Thus, the function $(Y_1+Y_2)/((Y_1+Y_2)/\min(X_1,X_2)+1)$ becomes $T/((T/Z)+1) = TZ/(T+Z)$ which is actually the harmonic mean of T and Z. Moreover, it is not hard to find the PDFs $f_T(t)$ of T and $f_Z(z)$ of Z

$$f_T(t) = \frac{e^{-\frac{t}{b_1}} - e^{-\frac{t}{b_2}}}{b_1-b_2}, \quad f_Z(z) = \left(\frac{1}{a_1}+\frac{1}{a_2}\right)e^{-\left(\frac{1}{a_1}+\frac{1}{a_2}\right)z}. \quad (17)$$

By using the results in [11], it is not hard to find $\mathcal{M}_2(s;a_1,a_2,b_1,b_2)$ in (15). □

Based on Lemma 2, one can easily find the MGF $\mathcal{M}^L(s)$ of γ^L and it is given by

$$\mathcal{M}^L(s) = \mathcal{M}_2\left(\frac{s}{\sigma_n^2}; E_s\Omega_{h_1}, E_s\Omega_{h_2}, E_{r_1}\Omega_{f_1}, E_{r_2}\Omega_{f_2}\right). \quad (18)$$

The MGF $\mathcal{M}^L(s)$ enables us to find an upper bound of P_b as in the following theorem.

Theorem 2: When M-QAM is used as the modulation scheme, the average BER P_b can be upper-bounded by

$$P_b \leq P_b^U = \frac{2}{\pi\sqrt{M}\log_2 M} \sum_{j=1}^{\log_2\sqrt{M}} \left\{ \sum_{i=0}^{(1-2^{-j})\sqrt{M}-1} A_{j,i}(M) \times \int_{\theta=0}^{\frac{\pi}{2}} \mathcal{M}^L\left(-\frac{3(2i+1)^2}{2(M-1)\sin^2\theta}\right) d\theta \right\}. \quad (19)$$

Proof: The proof is the same as that of Theorem 1, except $\mathcal{M}^L(s)$ is used in order to obtain an upper bound. □

The upper bound P_b^U also just contains a finite integration, and hence, it is not hard to compute. Moreover, as we expected, P_b^U is a very tight bound of the average BER P_b when Ω_{h_k} is much larger than Ω_{f_k}. This is because the denominator of (6) is dominantly decided by the constant one for this special case. As a result, replacing $|h_1|^2$ and $|h_2|^2$ by $\min(|h_1|^2,|h_2|^2)$ in (14) only slightly reduces the value of $\gamma(\rho_1,\rho_2)$, and hence, P_b^U is very tight to P_b. Recall that the lower bound P_b^L is very tight to P_b except when Ω_{h_k} is much larger than Ω_{f_k}. Therefore, depending on the values of Ω_{h_k} and Ω_{f_k}, one can always use either P_b^L or P_b^U in order to tightly bound the average BER P_b for every possible scenario.

C. Diversity order of the distributed Alamouti's code when the CSI-assisted relays use ρ_k

In the following theorem, we show that the distributed Alamouti's code achieves diversity order one when the relays use ρ_k of (5).

Theorem 3: In a cooperative network with two CSI-assisted relays, the distributed Alamouti's code achieves diversity order one when the relays use ρ_k of (5) as the amplifying coefficient.

Proof: See Appendix B. □

Note that, in the proof of Theorem 3, we use the exact SNR of (1), not the approximate SNR of (6). Therefore, the result of Theorem 3 is exact. Actually, the diversity order of the distributed Alamouti's code can intuitively be inferred from its approximate SNR $\gamma(\rho_1, \rho_2)$ in (6). When the channel from S to R_1 is in deep fading, i.e. when $|h_1|^2$ is very small, the denominator of (6) may go to infinity, and hence, $\gamma(\rho_1, \rho_2)$ may be very small. Similarly, when $|h_2|^2$ is very small, $\gamma(\rho_1, \rho_2)$ may go to zero as well. That is, the failure of either h_1 or h_2 will make the approximate SNR at the destination very small, which implies the diversity order is just one.

Furthermore, in a general cooperative network with more than two relays, we conjecture that the DSTBCs proposed in [2] achieve only diversity order one as well when the amplifying coefficient proposed in [1] is used at the relays.[3] Although the analytical proof is very difficult, the simulated BER results in Section V will suggest that the diversity order is one. However, the simulation results should be interpreted cautiously, because the asymptotic slope of the BER may not appear at typical BER values.

IV. A New Threshold-Based Amplifying Coefficient for the Distributed Alamouti's Code with CSI-Assisted Relays

In Section III, we showed that the distributed Alamouti's code achieved only diversity order one when the relays adopted the amplifying coefficient ρ_k of (5). In order to solve this problem, one may use the blind relaying coefficient; however, this raises another problem, a very large (possibly infinite in theory) PAPR. In this section, to address those problems, we propose a new amplifying coefficient $\tilde{\rho}_k$ as follows:

$$\tilde{\rho}_k = \sqrt{\frac{E_{rk}}{E_s \max(|h_k|^2, \alpha_k) + \sigma_n^2}} = \sqrt{\frac{E_{rk}}{\max(E_s|h_k|^2 + \sigma_n^2, E_s\alpha_k + \sigma_n^2)}}, \tag{20}$$

where $\alpha_k > 0$ can be seen as a threshold for $|h_k|^2$ and the choice of α_k will be discussed in detail later. If the received symbol power is greater than a threshold, i.e. $E_s|h_k|^2 + \sigma_n^2 > E_s\alpha_k + \sigma_n^2$, then $\tilde{\rho}_k$ becomes the same as the CSI-assisted relaying coefficient ρ_k of (5); if the received symbol power is smaller than or equal to a threshold, i.e. $E_s|h_k|^2 + \sigma_n^2 \leq E_s\alpha_k + \sigma_n^2$, then $\tilde{\rho}_k$ becomes the same as the blind relaying coefficient [2], [8], and [9]. This new amplifying coefficient enjoys two benefits: 1) it enhances the power efficiency by guaranteeing the PAPR at each relay to stay within a certain range; 2) it also makes the distributed Alamouti's code achieve the full diversity order two. Firstly, it is easy to check that the transmission power at the k-th relay is always less than or equal to E_{rk} when $\tilde{\rho}_k$ is used. That is, $E_{\max} = E_{rk}$; also, E_{avg} is given by $E_{\text{avg}} = \mathrm{E}\big[E_{rk}(E_s|h_k|^2 + \sigma_n^2)/(E_s \max[|h_k|^2, \alpha_k] + \sigma_n^2)\big] \approx E_{rk}$. Thus, the PAPR remains within a certain (controllable small) value. Consequently, the new amplifying coefficient $\tilde{\rho}_k$ enhances the power efficiency at each relay. Furthermore, we will show that the use of $\tilde{\rho}_k$ also makes the distributed Alamouti's code achieve the full diversity order. This is the topic of the next subsection.

A. Diversity order of the distributed Alamouti's code when the CSI-assisted relays use $\tilde{\rho}_k$

In this subsection, we show that the distributed Alamouti's code can achieve the full diversity order when the relays use $\tilde{\rho}_k$. In this circumstance, the instantaneous SNR $\tilde{\gamma}(\alpha_1, \alpha_2)$ of $\hat{x}_1$ or $\hat{x}_2$ is given by

$$\begin{aligned}\tilde{\gamma}&(\alpha_1, \alpha_2)\\ &= \gamma(\tilde{\rho}_1, \tilde{\rho}_2)\\ &= \frac{E_s\left(\frac{E_{r1}|f_1h_1|^2}{E_s\max(|h_1|^2,\alpha_1)+\sigma_n^2} + \frac{E_{r2}|f_2h_2|^2}{E_s\max(|h_2|^2,\alpha_2)+\sigma_n^2}\right)}{\sigma_n^2\left(\frac{E_{r1}|f_1|^2}{E_s\max(|h_1|^2,\alpha_1)+\sigma_n^2} + \frac{E_{r2}|f_2|^2}{E_s\max(|h_2|^2,\alpha_2)+\sigma_n^2} + 1\right)}.\end{aligned} \tag{21}$$

Thus, the conditional BER is given by $P_b(\tilde{\gamma}(\alpha_1, \alpha_2))$, and the average BER is given by $\tilde{P}_b = \mathrm{E}[P_b(\tilde{\gamma}(\alpha_1, \alpha_2))]$. We show the diversity order by deriving an upper bound of $\tilde{P}_b$. To this end, we develop the following lemma.

Lemma 3: Assume X, Y_1, and Y_2 are exponential random variables with means a, b_1, and b_2, respectively. The MGF $\mathcal{M}_3(s; a, b_1, b_2)$ of the function $XY_1/(Y_1 + Y_2 + 1)$ is given as follows:

$$\mathcal{M}_3(s; a, b_1, b_2) = 1 + asH\left(\frac{b_2}{b_1}, -as, \frac{1}{b_1}\right), \tag{22}$$

where the function $H(x, y, z)$ is given by

$$\begin{aligned}H(x,y,z) = &\frac{1}{(x+y-1)^2(1-y)}\\ &\times\Bigg[(1-y)(x+y-1) + e^{\frac{z}{x}}\mathrm{Ei}\left(-\frac{z}{x}\right)x(1-y)\\ &+ e^{\frac{z}{1-y}}\mathrm{Ei}\left(\frac{z}{-1+y}\right)(xz - (x+z)(1-y))\Bigg].\end{aligned} \tag{23}$$

Proof: See Appendix C. □

Based on Lemma 3, an upper bound of $\tilde{P}_b$ is derived in the following lemma.

Lemma 4: When M-QAM is used as the modulation scheme, the average BER $\tilde{P}_b$ can be upper-bounded by

$$\begin{aligned}\tilde{P}_b &\lesssim \tilde{P}_b^{UP}\\ &= \frac{2}{\pi\sqrt{M}\log_2 M}\sum_{j=1}^{\log_2\sqrt{M}}\sum_{i=0}^{(1-2^{-j})\sqrt{M}-1} A_{j,i}(M)\\ &\quad\times\tilde{\mathcal{M}}^L\left(-\frac{3(2i+1)^2}{M-1}\right),\end{aligned} \tag{24}$$

[3]Note that the DSTBCs proposed in [2] represent a large collection of distributed space-time codes and they have been used in many previous publications including [20]–[22].

where $\tilde{\mathcal{M}}^L(s) = \sum_{i=1}^{4} \mathcal{M}_{\tilde{\gamma}^{L\text{-}i}}(s)$, and the function $\mathcal{M}_{\tilde{\gamma}^{L\text{-}i}}(s)$ is given by

$$\mathcal{M}_{\tilde{\gamma}^{L\text{-}1}}(s) \approx \mathcal{M}_3\Big(s\frac{E_s}{\sigma_n^2};\Omega_{h_1},b_1,b_2\Big)\mathcal{M}_3\Big(s\frac{E_s}{\sigma_n^2};\Omega_{h_2},b_2,b_1\Big), \tag{25}$$

$$\mathcal{M}_{\tilde{\gamma}^{L\text{-}2}}(s) \lesssim \mathcal{M}_3\Big(s\frac{E_s}{\sigma_n^2};\Omega_{h_1},b_1,b_2\Big)\mathcal{M}_3\Big(s\frac{E_s\alpha_2}{\sigma_n^2};1,b_2,b_1\Big), \tag{26}$$

$$\mathcal{M}_{\tilde{\gamma}^{L\text{-}3}}(s) \lesssim \mathcal{M}_3\Big(s\frac{E_s\alpha_1}{\sigma_n^2};1,b_1,b_2\Big)\mathcal{M}_3\Big(s\frac{E_s}{\sigma_n^2};\Omega_{h_2},b_2,b_1\Big), \tag{27}$$

$$\mathcal{M}_{\tilde{\gamma}^{L\text{-}4}}(s) \lesssim \mathcal{M}_3\Big(s\frac{E_s\alpha_1}{\sigma_n^2};1,b_1,b_2\Big)\mathcal{M}_3\Big(s\frac{E_s\alpha_2}{\sigma_n^2};1,b_2,b_1\Big), \tag{28}$$

where $b_1 = E_{r1}\Omega_{f_1}/(E_s\alpha_1)$ and $b_2 = E_{r2}\Omega_{f_2}/(E_s\alpha_2)$.

Proof: See Appendix D. □

The upper bound $\tilde{P}_b^{UP}$ enables us to obtain the diversity order of the distributed Alamouti's code when the relays use $\tilde{\rho}_k$ as the amplifying coefficient and it is shown in the following theorem.

Theorem 4: In a cooperative network with two CSI-assisted relays, the distributed Alamouti's code achieves the full diversity order two when the relays use $\tilde{\rho}_k$ as the amplifying coefficient.

Proof: In order to show the diversity order, we assume $E_s = E_{r1} = E_{r2} = E$ and $\sigma_n^2 = 1$. Then it can be easily shown that

$$\lim_{E\to\infty} E^2 \tilde{\mathcal{M}}^L\left(-\frac{3(2i+1)^2}{M-1}\right) = C_2, \tag{29}$$

where $0 < C_2 < \infty$. That is, $\tilde{\mathcal{M}}^L\left(-3(2i+1)^2/(M-1)\right)$ behaves like $1/E^2$, when E is large. Thus, when E is large, $\tilde{P}_b^{UP}$ behaves like $1/E^2$. Since $\tilde{P}_b^{UP}$ is an upper bound of $\tilde{P}_b$, the average BER $\tilde{P}_b$ behaves like $1/E^2$ as well when E is large. That is, the diversity order of the distributed Alamouti's code is two when the CSI-assisted relays use $\tilde{\rho}_k$ as the amplifying coefficient. □

B. Amplifying schemes to determine the value of α_1 and α_2

The use of $\tilde{\rho}_k$ makes the distributed Alamouti's code achieve the full diversity order two as long as the threshold α_k is strictly positive, irrespective of the selection of α_k. For a small value α_k, however, the noise propagation may severely degrade the system performance in the practical SNR range. Therefore, the value of α_k should be determined properly in order to enhance the performance. In the remaining of this subsection, we propose four amplifying schemes to determine the value of α_k based on different CSI assumptions.

1) Amplifying Scheme I given channel variances: In order to optimize the value of α_k, it will be ideal to use the exact average BER $\tilde{P}_b$; but $\tilde{P}_b$ is too hard to obtain. Thus, we use upper bounds of $\tilde{P}_b$ to optimize α_k by using similar ideas in [2], [24], and [25]. It is possible to use the upper bound $\tilde{P}_b^{UP}$ of (24) to optimize α_k. In this paper, however, we adopt more tight upper bounds to optimize α_k. To this end, we first use the following well-known very accurate approximation [19] to obtain the lower bound $\tilde{P}_b$ in closed-form:

$$Q(x) \approx \frac{1}{12}e^{-\frac{1}{2}x^2} + \frac{1}{4}e^{-\frac{2}{3}x^2}. \tag{30}$$

Taking a step similar to (24), we obtain an upper bound $\tilde{P}_b^U$ as follows:

$$\begin{aligned}\tilde{P}_b &\lesssim \tilde{P}_b^U\\ &= \frac{2}{\sqrt{M}\log_2 M}\sum_{j=1}^{\log_2\sqrt{M}}\Bigg\{\sum_{i=0}^{(1-2^{-j})\sqrt{M}-1} A_{j,i}(M)\\ &\quad\times\left[\frac{1}{12}\tilde{\mathcal{M}}^L\left(-\frac{3(2i+1)^2}{2(M-1)}\right)+\frac{1}{4}\tilde{\mathcal{M}}^L\left(-\frac{2(2i+1)^2}{M-1}\right)\right]\Bigg\}.\end{aligned} \tag{31}$$

Then we determine α_k that minimizes the upper bound:

Amplifying Scheme I:

$$(\alpha_1,\alpha_2) = \arg\min_{\alpha_1>0,\alpha_2>0}\tilde{P}_b^U. \tag{32}$$

The scheme given in (32) is referred to as Amplifying Scheme I in this paper and it is optimum in the sense that it minimizes the upper bound $\tilde{P}_b^U$ given channel variances only. Note that the upper bound $\tilde{P}_b^U$ has been averaged over the instantaneous channel gains h_k and f_k. Thus, it only depends on the channel variances Ω_{h_k} and Ω_{f_k} which change very slowly. Thus, although the minimization in Amplifying Scheme I has to be solved numerically, the relays only need to conduct the minimization once in a long time and the computational loads at the relays may be negligible.

2) Amplifying Scheme II given instantaneous CSI for first hop: Amplifying Scheme I can greatly improve the performance of the distributed Alamouti's code with very low computational loads at the relays. However, it is more desirable to develop a scheme where α_k is optimized by exploiting the instantaneous channel coefficient h_k (not just channel variances). One can expect that the performance may be further improved by doing so. To this end, we take the expectation of the conditional BER $P_b(\tilde{\gamma}(\alpha_1,\alpha_2))$ over f_k only and upper-bound this expectation by using (31):

$$\mathrm{E}_{f_1,f_2}\left[P_b\left(\tilde{\gamma}(\alpha_1,\alpha_2)\right)\right] \lesssim \tilde{P}_b^U(h_1,h_2), \tag{33}$$

where $\tilde{P}_b^U(h_1,h_2)$ is obtained from (31) by replacing $\tilde{\mathcal{M}}^L(s)$ with $\tilde{\mathcal{M}}^U(s)$, which is given by

$$\begin{aligned}\tilde{\mathcal{M}}^U(s) &= \mathcal{M}_3\left(s\frac{E_s|h_1|^2}{\sigma_n^2};1,\tilde{\rho}_1^2\Omega_{f_1},\tilde{\rho}_2^2\Omega_{f_2}\right)\\ &\quad\times\mathcal{M}_3\left(s\frac{E_s|h_2|^2}{\sigma_n^2};1,\tilde{\rho}_2^2\Omega_{f_2},\tilde{\rho}_1^2\Omega_{f_1}\right).\end{aligned} \tag{34}$$

Then a new scheme to determine α_k is given as follows:

Amplifying Scheme II:

$$(\alpha_1,\alpha_2) = \arg\min_{\alpha_1>0,\alpha_2>0}\tilde{P}_b^U(h_1,h_2). \tag{35}$$

The scheme given in (35) is called Amplifying Scheme II in this paper and it is optimum in the sense that the upper bound $\tilde{P}_b^U(h_1,h_2)$ is minimized given instantaneous CSI for the first hop.[4] Numerical results will show that, compared to Amplifying Scheme I, Amplifying Scheme II indeed further improves the performance. This is because Amplifying Scheme II takes advantage of the instantaneous CSI available at the relays. However, the minimization in (35) must be solved numerically and it has to be done whenever the instantaneous channel gain h_k changes, because the upper bound $\tilde{P}_b^U(h_1, h_2)$ depends on h_k. Also, for Amplifying Scheme II, each relay requires the instantaneous CSI for the first hop. Thus, Amplifying Scheme II has higher computational complexity and signaling overhead than Amplifying Scheme I.

3) Amplifying Scheme III with closed-form solution: In a fast-fading environment, it may be hard to numerically perform the minimization in (35) whenever h_k changes. Thus, we develop another amplifying scheme which determines α_k by still exploiting h_k, but requires much less computational loads than Amplifying Scheme II. This is achieved by analyzing the property of the instantaneous SNR $\tilde{\gamma}(\alpha_1, \alpha_2)$ in (21). It can be shown that, when $0 < \alpha_1 < |h_1|^2$, $\tilde{\gamma}(\alpha_1, \alpha_2)$ is independent of α_1; while, when $\alpha_1 \geq |h_1|^2$, $\tilde{\gamma}(\alpha_1, \alpha_2)$ is decreasing with α_1 if and only if

$$E_{r2}|f_2|^2\left(|h_2|^2 - |h_1|^2\right) - E_s|h_1|^2 \max(|h_2|^2, \alpha_2) - |h_1|^2\sigma_n^2 < 0. \tag{36}$$

A sufficient condition for the inequality (36) is $|h_1|^2 > |h_2|^2$, and hence, the first relay must set $\alpha_1 = |h_1|^2$ when $|h_1|^2 > |h_2|^2$ in order to maximize $\tilde{\gamma}(\alpha_1, \alpha_2)$.

Then we show how the second relay should decide α_2 after the first relays sets $\alpha_1 = |h_1|^2$. When $|h_1|^2 > |h_2|^2$ and $\alpha_1 = |h_1|^2$, it can be shown that, if $0 < \alpha_2 < |h_2|^2$, $\tilde{\gamma}(|h_1|^2, \alpha_2)$ is independent of α_2; while, if $\alpha_2 \geq |h_2|^2$, $\tilde{\gamma}(|h_1|^2, \alpha_2)$ is decreasing with α_2 if and only if

$$\frac{\tilde{\gamma}_{s,1}\tilde{\gamma}_{1,d}}{\tilde{\gamma}_{s,1} + \tilde{\gamma}_{1,d} + 1} < \tilde{\gamma}_{s,2}, \tag{37}$$

where $\tilde{\gamma}_{s,k} = E_s|h_k|^2/\sigma_n^2$ and $\tilde{\gamma}_{k,d} = E_{rk}|f_k|^2/\sigma_n^2$. That is, when the inequality (37) is satisfied, the maximum value of $\tilde{\gamma}(|h_1|^2, \alpha_2)$ is $\tilde{\gamma}(|h_1|^2, |h_2|^2)$ and it is achieved by setting $\alpha_2 = |h_2|^2$; while, when the inequality (37) is not satisfied, the maximum value of $\tilde{\gamma}(|h_1|^2, \alpha_2)$ is $\tilde{\gamma}(|h_1|^2, \infty)$ and it is achieved by setting $\alpha_2 = \infty$. However, the second relay can not use (37) to decide α_2, because it requires $\tilde{\gamma}_{1,d}$ or equivalently f_1 which is not available at the second relay.

Although (37) can not be directly used to decide the value of α_2, it implies that, if $\tilde{\gamma}_{s,2}$ is very large, $\tilde{\gamma}(|h_1|^2, \alpha_2)$ is decreasing with α_2 with a higher probability, and hence, we should try to make its value close to $\tilde{\gamma}(|h_1|^2, |h_2|^2)$. On the other hand, when $\tilde{\gamma}_{s,2}$ is very small, $\tilde{\gamma}(|h_1|^2, \alpha_2)$ is increasing with α_2 with a higher probability, and hence, we should try to make its value close to $\tilde{\gamma}(|h_1|^2, \infty)$. Therefore, we let $\tilde{\gamma}(|h_1|^2, \alpha_2)$ equal to a combination of $\tilde{\gamma}(|h_1|^2, |h_2|^2)$ and $\tilde{\gamma}(|h_1|^2, \infty)$ as follows:

$$\begin{aligned}\tilde{\gamma}(|h_1|^2, \alpha_2) &= \left(1 - e^{-\tilde{\gamma}_{s,2}}\right)\tilde{\gamma}(|h_1|^2, |h_2|^2) \\ &\quad + e^{-\tilde{\gamma}_{s,2}}\tilde{\gamma}(|h_1|^2, \infty).\end{aligned} \tag{38}$$

It can be easily seen from (38) that the instantaneous SNR $\tilde{\gamma}(|h_1|^2, \alpha_2)$ will be very close to $\tilde{\gamma}(|h_1|^2, |h_2|^2)$ when $\tilde{\gamma}_{s,2}$ is very large. On the other hand, when $\tilde{\gamma}_{s,2}$ is very small, $\tilde{\gamma}(|h_1|^2, \alpha_2)$ will converge to $\tilde{\gamma}(|h_1|^2, \infty)$.[5]

The value of α_2 can be solved from (38) and it equals to α_2^* that is given by

$$\alpha_2^* = |h_2|^2 + \frac{\sigma_n^2}{E_s(e^{\tilde{\gamma}_{s,2}} - 1)}\left(1 + \tilde{\gamma}_{s,2} + \frac{\tilde{\gamma}_{2,d}(1 + \tilde{\gamma}_{s,1})}{\tilde{\gamma}_{s,1} + \tilde{\gamma}_{1,d} + 1}\right). \tag{39}$$

Note that α_2^* still depends on f_k through $\tilde{\gamma}_{k,d}$. This dependence can be removed by simply taking the expectation of α_2^* over f_k and it gives us

$$\begin{aligned}\bar{\alpha}_2^* &= \mathrm{E}_{f_1, f_2}[\alpha_2^*] \\ &= |h_2|^2 + \frac{\sigma_n^2}{E_s(e^{\tilde{\gamma}_{s,2}} - 1)}\Big[1 + \tilde{\gamma}_{s,2} \\ &\quad + (1 + \tilde{\gamma}_{s,1})\frac{E_{r2}\Omega_{f_2}}{E_{r1}\Omega_{f_1}} e^{\frac{\sigma_n^2(1+\tilde{\gamma}_{s,1})}{E_{r1}\Omega_{f_1}}}\,\mathrm{Ei}\Big(\frac{\sigma_n^2(1 + \tilde{\gamma}_{s,1})}{E_{r1}\Omega_{f_1}}\Big)\Big].\end{aligned} \tag{40}$$

Therefore, our amplifying scheme to determine α_k is given as follows:

Amplifying Scheme III:

$$(\alpha_1, \alpha_2) = \begin{cases} (|h_1|^2, \bar{\alpha}_2^*), & |h_1|^2 > |h_2|^2, \\ (\bar{\alpha}_1^*, |h_2|^2), & |h_2|^2 > |h_1|^2, \end{cases} \tag{41}$$

where $\bar{\alpha}_1^*$ can be obtained similarly as in (39) and (40). The scheme given in (41) is called Amplifying Scheme III in this paper. As in Amplifying Scheme II, for Amplifying Scheme III, each relay also requires the instantaneous CSI for the first hop. Compared to Amplifying Scheme II, however, Amplifying Scheme III has similar performance, because it is given in closed form, requiring no numerical computation.

4) Amplifying Scheme IV given instantaneous CSI for entire network: We finally consider the scenario where the relays have the CSI for the first and second hops; that is, both h_k and f_k are known at the relays. In this case, the inequality (37) can be used by the relays to optimize α_k. Based on (36) and (37), we have a new amplifying scheme as follows:

Amplifying Scheme IV:

$$\begin{aligned}&(\alpha_1, \alpha_2) \\ &= \begin{cases} (|h_1|^2, \infty), & |h_1|^2 > |h_2|^2, \frac{\tilde{\gamma}_{s,1}\tilde{\gamma}_{1,d}}{\tilde{\gamma}_{s,1}+\tilde{\gamma}_{1,d}+1} > \tilde{\gamma}_{s,2}, \\ (\infty, |h_2|^2), & |h_2|^2 > |h_1|^2, \frac{\tilde{\gamma}_{s,2}\tilde{\gamma}_{2,d}}{\tilde{\gamma}_{s,2}+\tilde{\gamma}_{2,d}+1} > \tilde{\gamma}_{s,1}, \\ (|h_1|^2, |h_2|^2), & \text{otherwise}. \end{cases}\end{aligned} \tag{42}$$

[4]Note that the upper bounds $\tilde{P}_b^U$ and $\tilde{P}_b^U(h_1, h_2)$ are not used to evaluate the BER performance of the distributed Alamouti's code, and hence, their tightness is not of our greatest concern. Those two bounds might not be tight bounds, but they enable us to propose Amplifying Schemes I and II, which can greatly improve the performance of the distributed Alamouti's code as suggested by numerical results.

[5]Instead of (38), one can let $\tilde{\gamma}(|h_1|^2, \alpha_2)$ equal to a combination of $\tilde{\gamma}(|h_1|^2, |h_2|^2)$ and $\tilde{\gamma}(|h_1|^2, \infty)$ in many other different ways. They may also make $\tilde{\gamma}(|h_1|^2, \alpha_2)$ very close to $\tilde{\gamma}(|h_1|^2, |h_2|^2)$, when $\tilde{\gamma}_{s,2}$ is very large, and make $\tilde{\gamma}(|h_1|^2, \alpha_2)$ converge to $\tilde{\gamma}(|h_1|^2, \infty)$, when $\tilde{\gamma}_{s,2}$ is very small. In this paper, however, we use (38), because it enables us to analytically derive α_2 and its expectation in closed-form. Moreover, using (38) also achieves very good performance as suggested by numerical results.

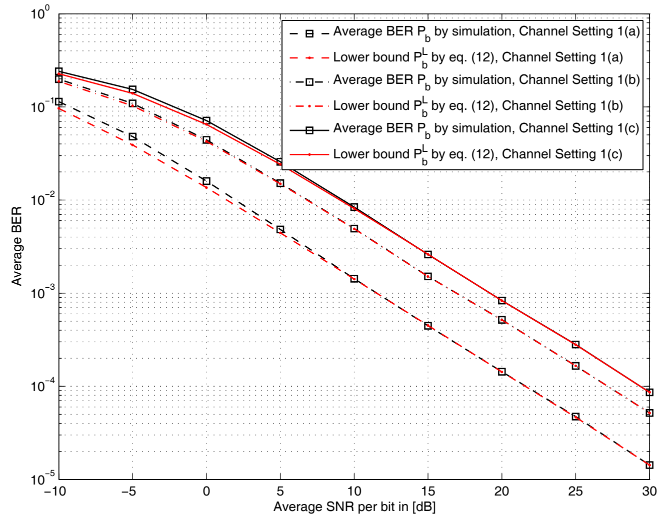

Fig. 2. Comparison of the lower bound P_b^L of (12) and the average BER P_b, 4-QAM. Channel Setting 1(a): $d_{s,1} = 0.5$, $d_{s,2} = 0.5$; Channel Setting 1(b): $d_{s,1} = 0.3$, $d_{s,2} = 0.7$; Channel Setting 1(c): $d_{s,1} = 0.7$, $d_{s,2} = 0.8$.

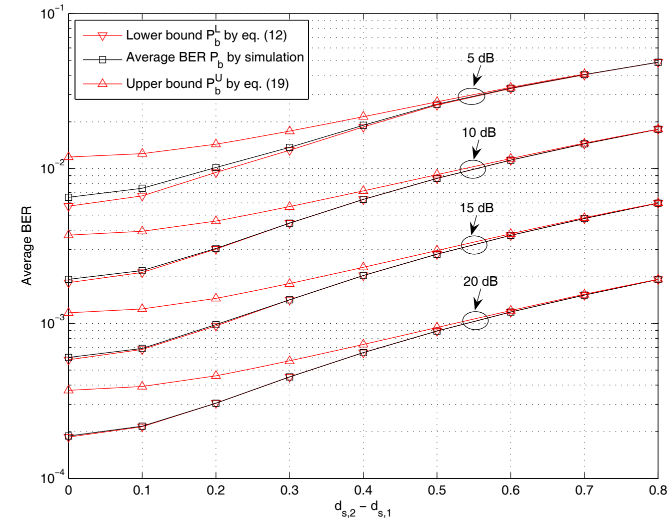

Fig. 3. Comparison of the lower bound P_b^L of (12), the upper bound of P_b^U (19), and the average BER P_b, 8-QAM and $d_{s,1} = d_{2,d}$.

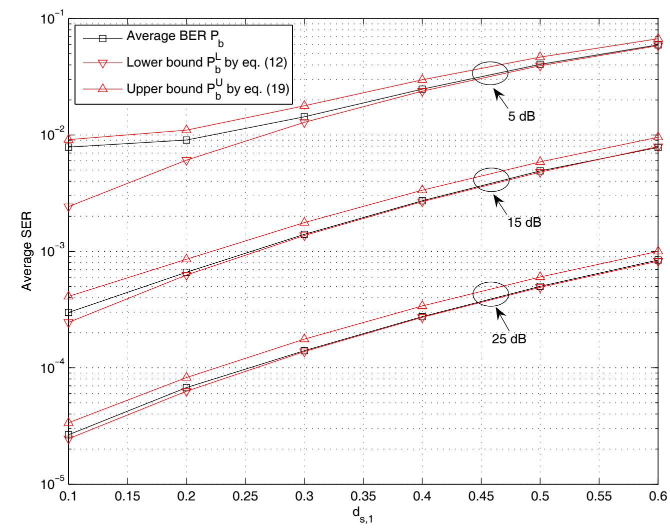

Fig. 4. Comparison of the lower bound P_b^L of (12), the upper bound of P_b^U (19), and the average BER P_b, 16-QAM and $d_{s,2} - d_{s,1} = 0.3$.

This method is referred to as Amplifying Scheme IV in this paper and it is optimum in the sense that it maximizes the instantaneous SNR $\tilde{\gamma}(\alpha_1, \alpha_2)$ given instantaneous CSI for the entire network. Note that for Amplifying Scheme IV, each relay requires the instantaneous CSI for entire network. Compared to Amplifying Schemes I–III, Amplifying Scheme IV achieves the best performance and it can be used as the performance benchmark. However, Amplifying Scheme IV may not be practical, because it requires a large amount of feedback overhead from the destination to the relays.

V. Numerical Results

We present some numerical results in this section. We use M-QAM as the modulation scheme. The source and the two relays have the same transmission powers, i.e. $E_s = E_{r1} = E_{r2} = E$. Thus, the average SNR per bit equals to $E/(\sigma_n^2 \log_2 M)$. In Subsection II-A, we modeled the channels h_k and f_k as follows: $h_k = \bar{h}_k \sqrt{d_{s,k}^{-\beta_{s,k}}}$ and $f_k = \bar{f}_k \sqrt{d_{k,d}^{-\beta_{k,d}}}$ with $\bar{h}_k \sim \mathcal{CN}(0,1)$ and $\bar{f}_k \sim \mathcal{CN}(0,1)$. We assume that the source, the relays, and the destination are located in a straight line. Furthermore, we let the reference distance equal to the distance from the source to the destination, and hence, $d_{s,k} = 1 - d_{k,d}$. We set the path loss exponents as $\beta_{s,k} = \beta_{k,d} = 4$ in order to model the wireless channels in an urban area. As a result, the channel variances Ω_{h_k} and Ω_{f_k} are purely decided by the locations of the relays, i.e. $\Omega_{h_k} = d_{s,k}^{-4}$ and $\Omega_{f_k} = d_{k,d}^{-4}$.

In Fig. 2, we compare the lower bound P_b^L in (12) with the average BER P_b. In order to test the tightness of P_b^L, we consider three channel settings by placing the relays at three different locations. It can be seen that P_b^L is very tight to P_b in all channel settings. In Fig. 3, we set $d_{s,1} = d_{2,d}$ and consider a wide range of channel settings by changing the distance $d_{s,2} - d_{s,1}$ between the two relays. One can see that P_b^L is very tight in all channel settings, but P_b^U is not very tight when the two relays are at the center of the source and the destination.

In Fig. 4, we fix the distance between the two relays by setting $d_{s,2} - d_{s,1} = 0.3$ and change the value of $d_{s,1}$. At high SNR range, P_b^L is still very tight. At low SNR range, P_b^L is not close to P_b when $d_{s,1}$ is small. However, P_b^U is tight to P_b for this case. Note that, when $d_{s,1}$ is small and $d_{s,2} - d_{s,1} = 0.3$, it actually implies that the value of Ω_{h_k} is much larger than that of Ω_{f_k}. Therefore, as we have discussed in Subsection III-B, P_b^U is a tight bound when the value of Ω_{h_k} is much larger than that of Ω_{f_k}.

From Fig. 4, one may argue that, when $d_{s,1} = 0.2$, P_b^U is not very close to P_b neither. We consider this special case as Channel Setting 2(c) in Fig. 5. We can see that P_b^U is at most 1 dB away from P_b, and hence, it still bounds the error performance of the distributed Alamouti's code well. Furthermore, in Channel Setting 2(a), we place the relays very close to the source, and hence, the value of Ω_{h_k} is much larger than that of Ω_{f_k}. For this special case, P_b^L may not be tight to

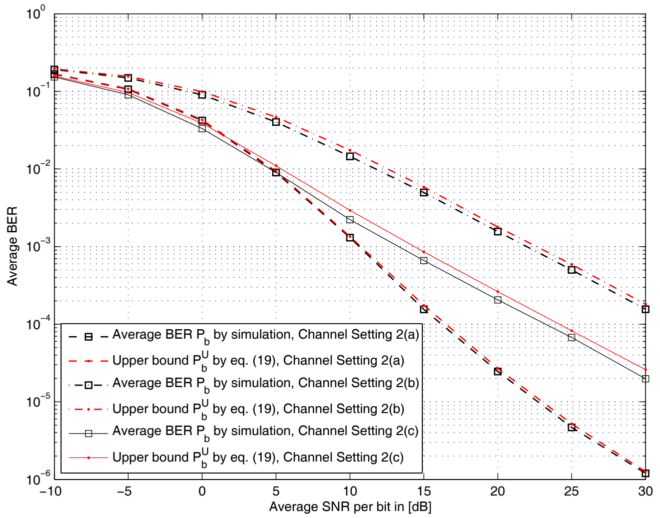

Fig. 5. Comparison of the upper bound P_b^U of (19) and the average BER P_b, 16-QAM. Channel Setting 2(a): $d_{s,1} = 0.2$, $d_{s,2} = 0.2$; Channel Setting 2(b): $d_{s,1} = 0.8$, $d_{s,2} = 0.5$; Channel Setting 2(c): $d_{s,1} = 0.2$, $d_{s,2} = 0.5$.

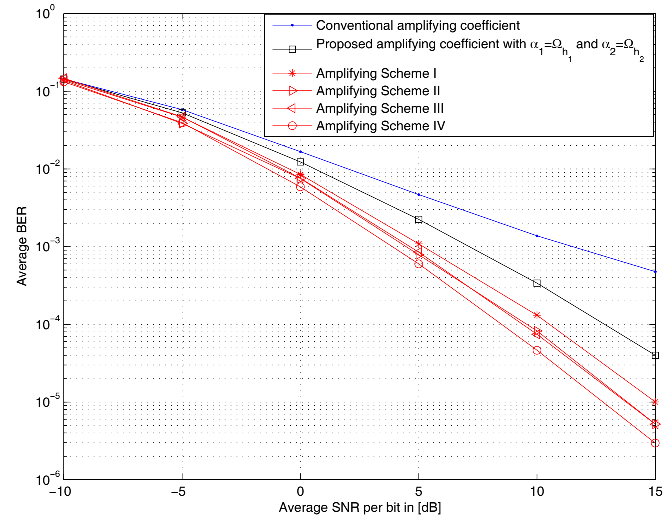

Fig. 7. Comparison of Amplifying Schemes I–IV , 4-QAM, $d_{s,1} = 0.5$, $d_{s,2} = 0.5$.

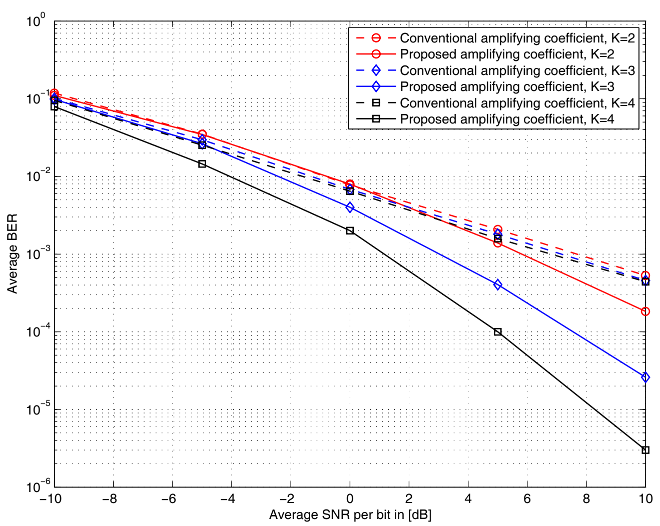

Fig. 6. Diversity order of the DSTBCs proposed by [2], BPSK, $d_{s,k} = 0.5$, $\alpha_k = \Omega_{h_k}$.

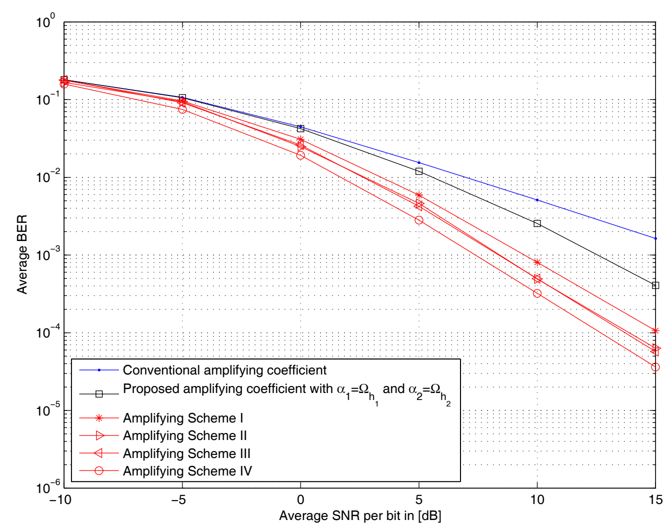

Fig. 8. Comparison of Amplifying Schemes I–IV, 8-QAM, $d_{s,1} = 1/3$, $d_{s,2} = 2/3$.

P_b as we have discussed in Subsection III-A and seen in Fig. 4; but Fig. 5 suggests that P_b^U is very tight to P_b. In all, our simulation results in Figs. 2–5 demonstrate that, irrespective of the values of Ω_{h_k} and Ω_{f_k}, we can always use either P_b^L or P_b^U in order to tightly bound P_b. Furthermore, the tightness of our bounds, especially the lower bound P_b^L, increases with the value of average SNR. At high SNR range, P_b^L is extremely close to P_b even when the value of Ω_{h_k} is much larger than that of Ω_{f_k}. Thus, it precisely evaluates the diversity order of the distributed Alamouti's code as we have discussed in Subsection III-C.

In Fig. 6, we examine the diversity order of the DSTBCs proposed by [2]. When the relays use the conventional amplifying coefficient ρ_k, it can be easily seen that the codes achieve only diversity order one. When the relays use our proposed amplifying coefficient $\tilde{\rho}_k$, however, Fig. 6 suggests that the codes achieve the full diversity order in the number of relays.

Lastly, in Figs. 7 and 8, we compare the performance of Amplifying Schemes I–IV proposed in Subsection IV-B. As performance benchmark, we include the average BER of the distributed Alamouti's code when the relays use the conventional amplifying coefficient ρ_k. We also present the average BER of the distributed Alamouti's code when the relays use the proposed amplifying coefficient $\tilde{\rho}_k$ and adopt $\alpha_k = \Omega_{h_k}$. In Figs. 7 and 8, when the relays use ρ_k, the code has the worst performance, because it achieves only diversity order one. When the relays use $\tilde{\rho}_k$, the code achieves the full diversity order two even by simply letting $\alpha_k = \Omega_{h_k}$. Furthermore, Amplifying Scheme I achieves much better performance compared to the case that the relays adopt $\alpha_k = \Omega_{h_k}$. Amplifying Scheme III further improves the performance by exploiting the CSI at the relays. Amplifying Scheme III has a similar performance as Amplifying Scheme

II and it has much lower computational loads. Among all the proposed schemes, Amplifying Scheme IV achieves the best performance; but it requires a large feedback overhead.

VI. Conclusion

In this paper, we analyze the average BER and the diversity order of the distributed Alamouti's code in dissimilar cooperative networks with CSI-assisted relays. We first let the relays adopt the amplifying coefficient ρ_k proposed in [1]. We derive lower and upper bounds of the average BER of the distributed Alamouti's code. The proposed bounds only contain integrations over finite range, and hence, can be easily calculated. Moreover, they can tightly bound the average BER irrespective of the values of the channel variances. Then we show that the code achieves only diversity order one when the relays use ρ_k. To address this problem, we propose a new threshold-based amplifying coefficient $\tilde{\rho}_k$ for the distributed Alamouti's code based on the work in [3]. This new amplifying coefficient enables the code achieve the full diversity order two. Based on three different CSI assumptions, we develop four amplifying schemes in order to determine the value of the threshold used in $\tilde{\rho}_k$. Numerical results demonstrate that the proposed schemes can enhance the performance of the distributed Alamouti's code substantially.

Appendix A
Proof of Lemma 1

We start the proof by rewriting the function $(Y_1 + Y_2)/\max(Y_1/X_1, Y_2/X_2)$ as

$$\frac{Y_1+Y_2}{\max\left(\frac{Y_1}{X_1},\frac{Y_2}{X_2}\right)} = \min\left(\left(1+\frac{Y_2}{Y_1}\right)X_1, \left(1+\frac{Y_1}{Y_2}\right)X_2\right). \tag{A.1}$$

Let $T = Y_2/Y_1$ and $Z = \min((1+T)X_1, (1+1/T)X_2)$. The probability density function (PDF) $f_T(t)$ of T is given by

$$f_T(t) = \frac{b_1 b_2}{(b_2+b_1 t)^2}. \tag{A.2}$$

When T is fixed, the conditional PDF $f_{(1+T)X_1|T}(x,t)$ of $(1+T)X_1$ is given by

$$f_{(1+T)X_1|T}(x,t) = \frac{1}{(1+t)a_1} e^{-\frac{x}{(1+t)a_1}}. \tag{A.3}$$

Similarly, the conditional PDF $f_{(1+\frac{1}{T})X_2|T}(x,t)$ of $(1+1/T)X_2$ is given by

$$f_{(1+\frac{1}{T})X_2|T}(x,t) = \frac{1}{\left(1+\frac{1}{t}\right)a_2} e^{-\frac{x}{\left(1+\frac{1}{t}\right)a_2}}. \tag{A.4}$$

Thus, the conditional PDF $f_{Z|T}(z,t)$ of Z is given by

$$f_{Z|T}(z,t) = \frac{a_2+a_1 t}{a_1 a_2(1+t)} e^{-\frac{a_2+a_1 t}{a_1 a_2 (1+t)} z}. \tag{A.5}$$

By taking the expectation over T, we can obtain the unconditional PDF $f_Z(z)$ of Z

$$\begin{aligned} f_Z(z) &= \mathrm{E}[f_{Z|T}(z,t)] \\ &= \frac{b_1 b_2}{a_1 a_2}\left[\frac{a_1-a_2}{b_1-b_2} f_Z^1(z) + \frac{a_2 b_1 - a_1 b_2}{b_1-b_2} f_Z^2(z)\right]. \end{aligned} \tag{A.6}$$

By using [15, pp. 337, 3.352.3], we obtain $f_Z^1(z)$ as follows:

$$\begin{aligned} f_Z^1(z) = \frac{e^{\frac{a_1 b_2 - a_2 b_1}{a_1 a_2 (b_1-b_2)} z}}{b_1-b_2} \Bigg[&\mathrm{Ei}\left(\frac{b_2(a_1-a_2)}{a_1 a_2 (b_1-b_2)} z\right) \\ &- \mathrm{Ei}\left(\frac{b_1(a_1-a_2)}{a_1 a_2(b_1-b_2)} z\right)\Bigg]. \end{aligned} \tag{A.7}$$

By integration by parts and using [15, pp. 337, 3.352.1], the function $f_Z^2(z)$ is given by

$$\begin{aligned} &f_Z^2(z) \\ &= \frac{e^{-\frac{z}{a_1}}}{b_2(b_1-b_2)} - \frac{e^{-\frac{z}{a_2}}}{b_1(b_1-b_2)} \\ &+ \left(\frac{1}{a_2}-\frac{1}{a_1}\right)\frac{z}{(b_2-b_1)^2} e^{\frac{a_1 b_2 - a_2 b_1}{a_1 a_2 (b_1-b_2)} z} \mathrm{Ei}\left(\frac{b_1(a_1-a_2)}{a_1 a_2 (b_1-b_2)} z\right) \\ &+ \left(\frac{1}{a_1}-\frac{1}{a_2}\right)\frac{z}{(b_2-b_1)^2} e^{\frac{a_1 b_2 - a_2 b_1}{a_1 a_2 (b_1-b_2)} z} \mathrm{Ei}\left(\frac{b_2(a_1-a_2)}{a_1 a_2 (b_1-b_2)} z\right). \end{aligned} \tag{A.8}$$

By definition, the MGF $\mathcal{M}_1(s; a_1, a_2, b_1, b_2)$ is given by

$$\begin{aligned} \mathcal{M}_1(s;a_1,a_2,b_1,b_2) = &\frac{b_1 b_2}{a_1 a_2}\left[\frac{a_1-a_2}{b_1-b_2}\int_0^\infty e^{sz} f_Z^1(z) dz \right. \\ &\left. + \frac{a_2 b_1 - a_1 b_2}{b_1-b_2}\int_0^\infty e^{sz} f_Z^2(z) dz\right]. \end{aligned} \tag{A.9}$$

With the help of [15, pp. 632, 6.227.1] and [15, pp. 633, 6.228], the integration involved in (A.9) can be solved and the final expression of $\mathcal{M}_1(s; a_1, a_2, b_1, b_2)$ is given by (8).

Appendix B
Proof of Theorem 3

We first present an upper bound of the exact SNR $\gamma(\rho_1, \rho_2)$ of (1) as follows:

$$\begin{aligned} \gamma(\rho_1,\rho_2) &< \frac{E_s}{\sigma_n^2}\left(\frac{\frac{E_{r1}|f_1|^2}{E_s} + \frac{E_{r2}|f_2|^2}{E_s}}{\frac{E_{r1}|f_1|^2}{E_s|h_1|^2+\sigma_n^2} + \frac{E_{r2}|f_2|^2}{E_s|h_2|^2+\sigma_n^2}}\right) &\text{(B.1)} \\ &< \frac{E_s}{\sigma_n^2}\left(\frac{\frac{E_{r1}|f_1|^2}{E_s} + \frac{E_{r2}|f_2|^2}{E_s}}{\frac{E_{r1}|f_1|^2}{E_s|h_1|^2+\sigma_n^2}}\right) &\text{(B.2)} \\ &= \left(1+\frac{E_{r2}|f_2|^2}{E_{r1}|f_1|^2}\right)\left(1+\frac{E_s|h_1|^2}{\sigma_n^2}\right) \\ &=: \gamma^{UP}. &\text{(B.3)} \end{aligned}$$

We let X, Y_1, and Y_2 denote exponential random variables with means a, b_1, and b_2, respectively. We now derive the MGF $\mathcal{M}_B(s; a, b_1, b_2)$ of the function $(1 + Y_2/Y_1)(1 + X)$. It can be shown that the PDF $f_{1+X}(x)$ of $1 + X$ is given by $f_{1+X}(x) = e^{-(x-1)/a}/a$ for $x \geq 1$; using (A.2), it can be shown that the PDF $f_{1+Y_2/Y_1}(t)$ of $1 + Y_2/Y_1$ is given by $f_{1+Y_2/Y_1}(t) = b/(t-1+b)^2$ with $b = b_2/b_1$ for $t \geq 1$.

Therefore, the MGF $\mathcal{M}_B(s;a,b_1,b_2)$ is given by

$$\begin{aligned}\mathcal{M}_B(s;a,b_1,b_2)\\ &= \int_{t=1}^{\infty}\int_{x=1}^{\infty} e^{stx} f_{1+X_1}(x) f_{1+Y_2/Y_1}(t)dxdt && \text{(B.4)}\\ &= \int_{1}^{\infty}\frac{e^{st}}{1-ast} f_{1+Y_2/Y_1}(t)dt && \text{(B.5)}\\ &= \frac{e^s}{(as-abs-1)^2}\Big(as-abs-1-abse^{\frac{1}{a}-s}\mathrm{Ei}\big(s-\frac{1}{a}\big)\\ &\quad - bs(as-abs-1-a)e^{-bs}\mathrm{Ei}(bs)\Big). && \text{(B.6)}\end{aligned}$$

Using (B.3) and (B.6), the MGF $\mathcal{M}^{UP}(s)$ of γ^{UP} can be easily derived, and it is given by

$$\mathcal{M}^{UP}(s) = \mathcal{M}_B\left(\frac{s}{\sigma_n^2}; E_s\Omega_{h_1}, E_{r_1}\Omega_{f_1}, E_{r_2}\Omega_{f_2}\right). \quad \text{(B.7)}$$

With a simple modification of [17. eq. (8)], one can obtain a lower bound of the Q-function as follows:

$$Q(x) \geq \sum_{i=1}^{N}\frac{\theta_i-\theta_{i-1}}{\pi} e^{\left(-\frac{x^2}{2\sin\theta_{i-1}^2}\right)}, \quad \text{(B.8)}$$

where $0=\theta_0 \leq \theta_1 \cdots \leq \theta_N = \pi/2$. For $N=2$ and $\theta_1 = \pi/4$, $Q(x)$ of (B.8) is lower-bounded by $Q(x) \geq \frac{1}{4}e^{-x^2}$. Taking a step similar to (12), the average BER P_b can be lower-bounded by

$$\begin{aligned}P_b \geq P_b^{LB} = \frac{1}{2\pi\sqrt{M}\log_2 M}\sum_{j=1}^{\log_2\sqrt{M}}\sum_{i=0}^{(1-2^{-j})\sqrt{M}-1}\\ A_{j,i}(M)\mathcal{M}^{UP}\left(-\frac{3(2i+1)^2}{M-1}\right). \quad \text{(B.9)}\end{aligned}$$

For simplicity, we assume $E_s = E_{r1} = E_{r2} = E$ and $\sigma_n^2 = 1$. Note that this assumption does not change the diversity order of the code. When E goes to infinity, we have

$$\lim_{E\to\infty} E\mathcal{M}^{UP}\left(-\frac{3(2i+1)^2}{M-1}\right) = C_1, \quad \text{(B.10)}$$

where $0 < C_1 < \infty$. That is, $\mathcal{M}^{UP}\left(-3(2i+1)^2/(M-1)\right)$ behaves like $1/E$, when E is large. Thus, when E is large, the lower bound P_b^{LB} decays with E as $1/E$. Since P_b^{LB} is a lower bound of P_b, the average BER P_b also decays with E as $1/E$. That is, the diversity order of the distributed Alamouti's code is just one when the relays use ρ_k as the amplifying coefficient.

Appendix C

Proof of Lemma 3

Let $T = Y_1/(Y_1+Y_2+1)$ and the cumulative density function (CDF) $F_T(t)$ of T is given by

$$F_T(t) = \begin{cases} 1-\frac{e^{-\frac{t}{b_1(1-t)}}}{\frac{b_2 t}{b_1(1-t)}+1}, & 0 \leq t \leq 1\\ 1, & t \geq 1\end{cases}. \quad \text{(C.1)}$$

Furthermore, we find the following integration

$$\begin{aligned}&\int_0^1 \frac{e^{-z\frac{t}{(1-t)}}}{\frac{xt}{(1-t)}+1}\frac{1}{(1-yt)^2}dt\\ &\overset{\frac{t}{1-t}=w}{=} \int_0^{\infty}\frac{e^{-zw}}{(xw+1)((1-y)w+1)^2}dw\\ &= H(x,y,z), && \text{(C.2)}\end{aligned}$$

where the last step is done by partial fraction and using [15, pp. 337, 3.352.4, 3.353.3]. Let $f_T(t)$ denote the PDF of T, then $\mathcal{M}_3(s;a,b_1,b_2)$ is given by

$$\begin{aligned}\mathcal{M}_3(s;a,b_1,b_2) &= \int_0^1\int_0^{\infty} e^{sxt}\frac{1}{a}e^{-\frac{x}{a}} f_T(t)dxdt && \text{(C.3)}\\ &= \int_0^1 \frac{1}{1-ast}dF_T(t) && \text{(C.4)}\\ &= \frac{F_T(t)}{1-ast}\Big|_{t=0}^{1} - \int_0^1 F_T(t)d\frac{1}{1-ast} && \text{(C.5)}\\ &= 1 + asH\left(\frac{b_2}{b_1}, -as, \frac{1}{b_1}\right), && \text{(C.6)}\end{aligned}$$

where the last step is done by integration by parts and using (C.2).

Appendix D

Proof of Lemma 4

Since $E_s\max(|h_1|^2,\alpha_1)+\sigma_n^2 > E_s\max(|h_1|^2,\alpha_1)$ and $E_s\max(|h_1|^2,\alpha_1)+\sigma_n^2 > E_s\alpha_1$ for $i=1,2$, the instantaneous SNR $\tilde{\gamma}(\alpha_1,\alpha_2)$ of (21) can be lower-bounded by

$$\begin{aligned}\tilde{\gamma}(\alpha_1,\alpha_2) &> \frac{E_s\left(\frac{E_{r1}|f_1h_1|^2}{E_s\max(|h_1|^2,\alpha_1)}+\frac{E_{r2}|f_2h_2|^2}{E_s\max(|h_2|^2,\alpha_2)}\right)}{\sigma_n^2\left(\frac{E_{r1}|f_1|^2}{E_s\alpha_1}+\frac{E_{r2}|f_2|^2}{E_s\alpha_2}+1\right)}\\ &=: \tilde{\gamma}^L. && \text{(D.1)}\end{aligned}$$

As a result, the average BER $\tilde{P}_b$ is upper-bounded by $\mathrm{E}\left[P_b(\tilde{\gamma}^L)\right]$. It is hard to obtain the exact value of $\mathrm{E}\left[P_b(\tilde{\gamma}^L)\right]$; but, in order to show the diversity order, it is sufficient to derive an upper bound of this expectation. To this end, we first develop the following inequality

$$\begin{aligned}\mathrm{E}\left[Q\left(g\sqrt{\tilde{\gamma}^L}\right)\right] &< \mathrm{E}\left[Q\left(g\sqrt{\tilde{\gamma}^{L\text{-}1}}\right)\right] + \mathrm{E}\left[Q\left(g\sqrt{\tilde{\gamma}^{L\text{-}2}}\right)\right]\\ &\quad + \mathrm{E}\left[Q\left(g\sqrt{\tilde{\gamma}^{L\text{-}3}}\right)\right] + \mathrm{E}\left[Q\left(g\sqrt{\tilde{\gamma}^{L\text{-}4}}\right)\right], && \text{(D.2)}\end{aligned}$$

where g can be any positive constant. The inequality in (D.2) is obtained by making all the integration limits from zero to ∞. Moreover, $\tilde{\gamma}^{L\text{-}i}$ is given by

$$\tilde{\gamma}^{L\text{-}1} = \frac{E_s\left(\frac{E_{r1}|f_1h_1|^2}{E_s\alpha_1}+\frac{E_{r2}|f_2h_2|^2}{E_s\alpha_2}\right)}{\sigma_n^2\left(\frac{E_{r1}|f_1|^2}{E_s\alpha_1}+\frac{E_{r2}|f_2|^2}{E_s\alpha_2}+1\right)},$$

$$\tilde{\gamma}^{L\text{-}2} = \frac{E_s\left(\frac{E_{r1}|f_1h_1|^2}{E_s\alpha_1}+\frac{E_{r2}|f_2|^2}{E_s}\right)}{\sigma_n^2\left(\frac{E_{r1}|f_1|^2}{E_s\alpha_1}+\frac{E_{r2}|f_2|^2}{E_s\alpha_2}+1\right)},$$

$$\tilde{\gamma}^{L\text{-}3} = \frac{E_s\left(\frac{E_{r1}|f_1|^2}{E_s} + \frac{E_{r2}|f_2h_2|^2}{E_s\alpha_2}\right)}{\sigma_n^2\left(\frac{E_{r1}|f_1|^2}{E_s\alpha_1} + \frac{E_{r2}|f_2|^2}{E_s\alpha_2} + 1\right)},$$

$$\tilde{\gamma}^{L\text{-}4} = \frac{E_s\left(\frac{E_{r1}|f_1|^2}{E_s} + \frac{E_{r2}|f_2|^2}{E_s}\right)}{\sigma_n^2\left(\frac{E_{r1}|f_1|^2}{E_s\alpha_1} + \frac{E_{r2}|f_2|^2}{E_s\alpha_2} + 1\right)}.$$

Secondly, we solve the expectations in (D.2) by analyzing the MGF of $\tilde{\gamma}^{L-i}$. We rewrite $\tilde{\gamma}^{L\text{-}1}$ as

$$\begin{aligned}\tilde{\gamma}^{L\text{-}1} &= \frac{E_s}{\sigma_n^2}\left(\frac{\frac{E_{r1}|f_1h_1|^2}{E_s\alpha_1}}{\frac{E_{r1}|f_1|^2}{E_s\alpha_1} + \frac{E_{r2}|f_2|^2}{E_s\alpha_2} + 1} + \frac{\frac{E_{r2}|f_2h_2|^2}{E_s\alpha_2}}{\frac{E_{r1}|f_1|^2}{E_s\alpha_1} + \frac{E_{r2}|f_2|^2}{E_s\alpha_2} + 1}\right)\\ &=: \tilde{\gamma}^{L\text{-}1a} + \tilde{\gamma}^{L\text{-}1b}. \qquad \text{(D.3)}\end{aligned}$$

The MGFs of $\tilde{\gamma}^{L\text{-}1a}$ and $\tilde{\gamma}^{L\text{-}1b}$ can be easily obtained by using Lemma 3.

Due to the common two random variables f_1 and f_2, two expressions $\tilde{\gamma}^{L\text{-}1a}$ and $\tilde{\gamma}^{L\text{-}1b}$ are dependent, which makes the analysis extremely difficult. In this paper, therefore, we ignore the dependency to make the analysis tractable. Then the MGF $\mathcal{M}_{\tilde{\gamma}^{L\text{-}1}}(s)$ of $\tilde{\gamma}^{L\text{-}1}$ is approximated by the product of the MGFs of $\tilde{\gamma}^{L\text{-}1a}$ and $\tilde{\gamma}^{L\text{-}1b}$ as in (25).

Then we rewrite $\tilde{\gamma}^{L\text{-}2}$ in the following way

$$\begin{aligned}\tilde{\gamma}^{L\text{-}2} &= \frac{E_s}{\sigma_n^2}\left(\frac{\frac{E_{r1}|f_1h_1|^2}{E_s\alpha_1}}{\frac{E_{r1}|f_1|^2}{E_s\alpha_1} + \frac{E_{r2}|f_2|^2}{E_s\alpha_2} + 1} + \frac{\frac{E_{r2}|f_2|^2}{E_s}}{\frac{E_{r1}|f_1|^2}{E_s\alpha_1} + \frac{E_{r2}|f_2|^2}{E_s\alpha_2} + 1}\right)\\ &=: \tilde{\gamma}^{L\text{-}2a} + \tilde{\gamma}^{L\text{-}2b}. \qquad \text{(D.4)}\end{aligned}$$

The MGF of $\tilde{\gamma}^{L\text{-}2a}$ can be easily obtained by using Lemma 3. The MGF $\mathcal{M}_{\tilde{\gamma}^{L\text{-}2b}}(s)$ of $\tilde{\gamma}^{L\text{-}2b}$ can be upper-bounded by

$$\begin{aligned}\mathcal{M}_{\tilde{\gamma}^{L\text{-}2b}}(s) &= \int_0^1 e^{sx} f(x)dx\\ &< \int_0^1 \frac{1}{1-sx} dF(x)\\ &= \mathcal{M}_3\left(s\frac{E_s\alpha_2}{\sigma_n^2}; 1, b_2, b_1\right), \qquad \text{(D.5)}\end{aligned}$$

where $f(x)$ and $F(x)$ are the PDF and CDF of $\tilde{\gamma}^{L\text{-}2b}$, respectively. In (D.5), the inequality is due to $e^{sx} < 1/(1-sx)$ when $s < 0$ and the last step is by using Lemma 3. We still ignore the dependency between $\tilde{\gamma}^{L\text{-}2a}$ and $\tilde{\gamma}^{L\text{-}2b}$. Thus, the MGF $\mathcal{M}_{\tilde{\gamma}^{L\text{-}2}}(s)$ of $\tilde{\gamma}^{L\text{-}2}$ is upper-bounded by (26). By following a similar way, the MGFs $\mathcal{M}_{\tilde{\gamma}^{L\text{-}3}}(s)$ and $\mathcal{M}_{\tilde{\gamma}^{L\text{-}4}}(s)$ of $\tilde{\gamma}^{L\text{-}3}$ and $\tilde{\gamma}^{L\text{-}3}$ are upper-bounded by (27) and (28), respectively.

Lastly, based on (30), (D.2), and (25)–(28), the expectation $\mathrm{E}\left[Q\left(g\sqrt{\tilde{\gamma}^L}\right)\right]$ can be upper-bounded as follows:

$$\mathrm{E}\left[Q\left(g\sqrt{\tilde{\gamma}^L}\right)\right] \le \tilde{\mathcal{M}}^L\left(-\frac{1}{2}g^2\right), \qquad \text{(D.6)}$$

where we use the Chernoff-Rubin bound for the Q-function [17. eq. (4)] : $Q(x) \le e^{-x^2/2}$. In the above equation, $\tilde{\mathcal{M}}^L(s)$ is given by $\tilde{\mathcal{M}}^L(s) = \sum_{i=1}^4 \mathcal{M}_{\tilde{\gamma}^{L\text{-}i}}(s)$. Based on (2)–(4), (D.6), and Craig's formula, the expectation $\mathrm{E}\left[P_b(\tilde{\gamma}^L)\right]$ can be upper-bounded by $\mathrm{E}\left[P_b(\tilde{\gamma}^L)\right] \le \tilde{P}_b^{UP}$. Moreover, since $\tilde{P}_b$ is upper-bounded by $\mathrm{E}\left[P_b(\tilde{\gamma}^L)\right]$, we conclude that the average BER $\tilde{P}_b$ is upper-bounded by $\tilde{P}_b^{UP}$ as well.

References

[1] J. N. Laneman, D. N. C. Tse, and G. W. Wornell, "Cooperative diversity in wireless networks: efficient protocols and outage behavior," *IEEE Trans. Inf. Theory*, vol. 50, pp. 3062–3080, Dec. 2004.

[2] Y. Jing and B. Hassibi, "Distributed space-time coding in wireless relay networks," *IEEE Trans. Wireless Commun.*, vol. 5, pp. 3524–3536, Dec. 2006.

[3] M. O. Hasna and M.-S. Alouini, "A performance study of dual-hop transmissions with fixed gain relays," *IEEE Trans. Wireless Commun.,* vol. 3, pp. 1963–1968, Nov. 2004.

[4] Z. Yi and I.-M. Kim, "Joint optimization of relay-precoders and decoders with partial channel side information in cooperative networks," *IEEE J. Sel. Areas Commun.*, vol. 25, pp. 447–458, Feb. 2007.

[5] Z. Yi and I.-M. Kim, "Diversity order analysis of the decode-and-forward cooperative networks with relay selection," *IEEE Trans. Wireless Commun.*, vol. 7, pp. 1792–1799, May 2008.

[6] J. N. Laneman and G. W. Wornell, "Distributed space-time-coded protocols for exploiting cooperative diversity in wireless networks," *IEEE Trans. Inf. Theory*, vol. 49, pp. 2415–2425, Oct. 2003.

[7] Z. Yi and I.-M. Kim, "Single-symbol ML decodable distributed STBCs for cooperative networks," *IEEE Trans. Inf. Theory*, vol. 53, pp. 2977–2985, Aug. 2007.

[8] M. Ju, H.-K. Song, and I.-M. Kim, "Exact BER analysis of distributed Alamouti's code for cooperative diversity networks," *IEEE Trans. Commun.*, vol. 57, pp. 2380–2390, Aug. 2009.

[9] Z. Yi and I.-M. Kim, "Approximate BER expressions of distributed Alamouti's code in dissimilar cooperative networks with blind relays," *IEEE Trans. Commun.,* vol. 57, pp. 3571–3578, Dec. 2009.

[10] P. A. Anghel and M. Kaveh, "On the performance of distributed space-time coding systems with one and two non-generative relays," *IEEE Trans. Wireless Commun.*, vol. 5, pp. 682–692, Mar. 2006.

[11] ——, "Exact symbol error probability of a cooperative network in a Rayleigh-fading environment," *IEEE Trans. Wireless Commun.*, vol. 3, pp. 1416–1421, Sep. 2004.

[12] A. Ribeiro, X. Cai, and G. B. Giannakis, "Symbol error probabilities for general cooperative links," *IEEE Trans. Wireless Commun.*, vol. 4, pp. 1264–1273, May 2005.

[13] K. G. Seddik, A. K. Sadek, W. Su, and K. J. R. Liu, "Outage analysis and optimal power allocation for multi-node amplify-and-forward relay networks," *IEEE Signal Process. Lett.*, vol. 14, pp. 377–380, June 2007.

[14] S. L. Miller and R. J. O'Dea, "Peak power and bandwidth efficient linear modulation," *IEEE Trans. Commun.*, vol. 46, pp. 1639–1648, Dec. 1998.

[15] I. S. Gradshteyn and I. M. Ryzhik, *Table of Integrals, Series, and Products*, 6th edition. Academic Press, 2000.

[16] T. S. Rappaport, *Wireless Communications: Principles and Practice*. Prentice Hall, 2002.

[17] K. Cho and D. Yoon, "On the general BER expression of one and two dimensional amplitude modulations," *IEEE Trans. Commun.,* vol. 50, pp. 1074–1080, July 2002.

[18] M. K. Simon and M.-S. Alouini, *Digital Communication over Fading Channels*, 2nd edition. Wiley, 2004.

[19] M. Chiani, D. Dardari, and M. K. Simon, "New exponential bounds and approximations for the compuation of error probability in fading channels," *IEEE Trans. Wireless Commun.,* vol. 2, pp. 840–845, July 2003.

[20] Y. Jing and H. Jafarkhani, "Using orthogonal and quasi-orthogonal designs in wireless relay networks," *IEEE Trans. Inf. Theory*, vol. 53, pp. 4106–4118, Nov. 2007.

[21] K. G. Seddik, A. K. Sadek, A. S. Ibrahim, and K. J. R. Liu, "Design criteria and performance analysis for distributed space-time coding," *IEEE Trans. Veh. Technol.,* vol. 57, pp. 2280–2292, July 2008.

[22] K.-C. Liang, X. Wang, and I. Berenguer, "Minimum error rate linear dispersion codes for cooperative relays," *IEEE Trans. Veh. Technol.,* vol. 56, pp. 2143–2157, July 2007.

[23] J. G. Proakis, *Digital Communications*, 4th edition. McGraw-Hill, 2001.

[24] Y. Zhao, R. Adve, and L. T. J, "Improving amplify-and-forward relay netwroks: optimal power allocation versus selection," *IEEE Trans. Wireless Commun.,* vol. 6, pp. 3114–3123, Aug. 2007.

[25] M. M. Fareed and M. Uysal, "BER-optimized power allocation for fading relay channels," *IEEE Trans. Wireless Commun.,* vol. 7, pp. 2350–2359, June 2008.

Zhihang Yi received his B.Eng. degree in Information Science and Electrical Engineering from Zhejiang University, China, in 2003, and M.Sc. and Ph.D. degrees from Queens University in 2005 and 2009, respectively. For his doctoral research at Queens, Dr. Yi investigated innovative relaying, MIMO, and OFDM technologies in wireless communication systems. Dr. Yi was the recipient of several research excellence awards during his graduate studies, including NSERC Industrial R&D Fellowship, NSERC Visiting Fellowship at Canadian Government Laboratories, Ontario Graduate Scholarships, and IEEE Kingston Section Ph.D. Research Excellence Award (Honorable Mention).

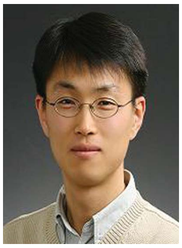

MinChul Ju received the B.S. degree in Electrical Engineering from Pohang University of Science and Technology (POSTECH), Pohang, Korea, in 1997, the M.S. degree in Electrical Engineering from Korea Advanced Institute of Science and Technology (KAIST), Taejon, Korea, in 1999, and the Ph.D. degree in Electrical and Computer Engineering from Queen's University, ON, Canada, in 2010. From 1999 to 2005, he was a researcher at Korea Electronics Technology Institute (KETI), Korea, where he was involved in many projects related with WPAN systems such as Bluetooth, IEEE802.15.3, IEEE802.11, and HomeRF. In 2010, he returned to the Wireless Network Research Center at KETI, where he is currently a Senior Researcher. His research interests are in the areas of opportunistic transmissions, cooperative networks, and synchronization in communication.

Hyoung-Kyu Song was born in CungCheongBukdo, Korea on May 14 in 1967. He received B.S., M.S., and Ph.D. degrees in electronic engineering from Yonsei University, Seoul, Korea, in 1990, 1992, and 1996, respectively. From 1996 to 2000 he had been managerial engineer in Korea Electronics Technology Institute (KETI), Korea. Since 2000 he has been an assistant professor of the Department of information and communications engineering, Sejong University, Seoul, Korea. His research interests include digital and data communications, information theory and their applications with an emphasis on mobile communications.

Il-Min Kim received the B.S. degree in electronics engineering from Yonsei University, Seoul, Korea, in 1996, and the M.S. and Ph.D. degrees in electrical engineering from the Korea Advanced Institute of Science and Technology (KAIST), Taejon, Korea, in 1998 and 2001, respectively. From October 2001 to August 2002 he was with the Dept. of Electrical Engineering and Computer Sciences at MIT, Cambridge, USA, and from September 2002 to June 2003 he was with the Dept. of Electrical Engineering at Harvard, Cambridge, USA, as a Postdoctoral Research Fellow. In July 2003, he joined the Dept. of Electrical and Computer Engineering at Queen's University, Kingston, Canada, where he is currently an Associate professor. His research interests include cooperative diversity networks, bidirectional communications, secure wireless communications, and heterogeneous wireless networks. He is currently serving as an Editor for IEEE TRANSACTIONS ON WIRELESS COMMUNICATIONS and the *Journal of Communications and Networks*.